

Influence of proton shell closure on production of new superheavy nuclei

A.N. Kuzmina¹, G.G. Adamian^{1,2}, and N.V. Antonenko¹

¹Bogoliubov Laboratory of Theoretical Physics, Joint Institute for Nuclear Research, 141980 Dubna, Russia

²Institute of Nuclear Physics, Tashkent, Uzbekistan

Abstract. The shell structure of nuclei with $Z > 104$ is studied with modified two-center shell model. Using macroscopic-microscopic approach, the mass excesses and Q_α -values are calculated and compared with available experimental data. Our calculations reveal quite strong shell effects at $Z = 120 - 126$ as well as at $N = 184$. If our predictions for the heaviest nuclei are correct then one can expect the production of evaporation residues with $Z \sim 120$ in the reactions $^{50}\text{Ti} + ^{249}\text{Cf}$ and $^{54}\text{Cr} + ^{248}\text{Cm}$ with the cross sections 23 and 10 fb, respectively. Nuclei with $Z = 120$ and $N = 178 - 182$ are expected to have Q_α about 11 MeV and life-time of 0.17 ms – 0.16 s.

1 Introduction

To find ways of synthesis and identification of superheavy nuclei, the study of their structure is necessary [1,2]. The stability of superheavy nuclei is related to the shell effects which are ruled by the mean field and the spin-orbit interaction. Existing microscopic-macroscopic approaches [3–5] supply the basis for the intensive calculations of the properties of heavy nuclei.

The aim of this work is to apply the microscopic-macroscopic approach based on the two-center shell model TCSM [6] to the SHN and to reveal the trends in the shell effects, nuclear binding energies, Q_α -values, quasiparticle states, and the evaporation residue cross sections with Z . The parameters of the TCSM were set so to describe the spins and parities of the ground state of known heavy nuclei (the rare earth nuclei, actinides, and some superheavy nuclei). This approach has been used in Ref. [7]. Note that the spectroscopic study of low-lying one- and two-quasiparticle states, and isomers in the heaviest nuclei [8–11] is up to date because of the problem of unambiguous identification of new superheavy nuclei [1, 12–14].

2 Modified TCSM

In our work, we use the shape parametrization adopted for the TCSM and use it for finding the single-particle levels in the ground state of the nucleus.

The contribution of an odd nucleon, occupying a single-particle state $|\mu\rangle$ with energy e_μ , to energy of a nucleus is described by the one-quasiparticle energy $\sqrt{(e_\mu - e_F)^2 + \Delta^2}$. Here, the Fermi energy e_F and the pairing-energy gap parameter Δ are calculated with the BCS approximation. Pairing interaction of the monopole type with strength parameters $G_p^n = (19.2 \mp 7.4 \frac{N-Z}{A})A^{-1}$ MeV [15] for neutrons and protons is used. For solving the pairing equations for e_F and Δ , the same prescription as in Ref. [15] is used. In the calculations of e_F and Δ the blocking effect [16] is not taken explicitly into consideration. To take it effectively into account in the calculations of one-quasiparticle excitations $E_\mu = \sqrt{(e_\mu - e_F)^2 + \Delta^2} - \sqrt{(e'_\mu - e_F)^2 + \Delta^2}$, where

e'_μ is the single-particle energy of occupied level below the Fermi level energies, we use the results of Ref. [16] where the reduction of Δ occurs by about factor of 0.85. Calculating the potential energy surface as a function of collective coordinates with the TCSM, we find the ground-state potential minimum in which the energies of the low-lying one-quasiparticle states are obtained.

The details of the calculations of binding energies of nuclei in the ground states are presented in Ref. [5,7].

3 Binding energies

For the calculations of the binding energies of nuclei in the ground states we suggest the following expression:

$$B(Z, A) = U(Z, A, \lambda_{gs}, \beta_{gs}) - a_v \left(1 - a_s \left(\frac{N-Z}{A} \right)^2 \right) A + W \left| \frac{N-Z}{A} \right| + \delta + c[(N-Z) - 58], \quad (1)$$

where $a_s = 1.778$, the Wigner constant $W = 30$ MeV, $c = 0.25$ MeV in the term correcting the charge-asymmetry energy, and the average pairing energy $\delta = 4.8/N^{1/3} + 4.8/Z^{1/3}$, $4.8/N^{1/3}$, $4.8/Z^{1/3}$, and 0 MeV for odd Z and N , even Z and odd N , odd Z and even N , and even Z and N , respectively.

4 Calculations

The calculated mass excesses M_{th} , neutron separation energies S_n , shell corrections E_{sh} , and Q_α -values you can see in [7] for nuclei with $105 \leq Z \leq 126$.

As seen in figure 1, the calculated Q_α are in a good, within 0.3 MeV, agreement with the available experimental Q_α^{exp} [1,2,12,17]. The shell at $N = 162$ is pronounced in our calculations as in Refs. [3,4]. The shell effects at $Z = 114$ and $N = 172 - 176$ provide rather weak dependence of Q_α on N . The strong role of the shell at $N = 184$ is reflected in the well pronounced minimum of Q_α .

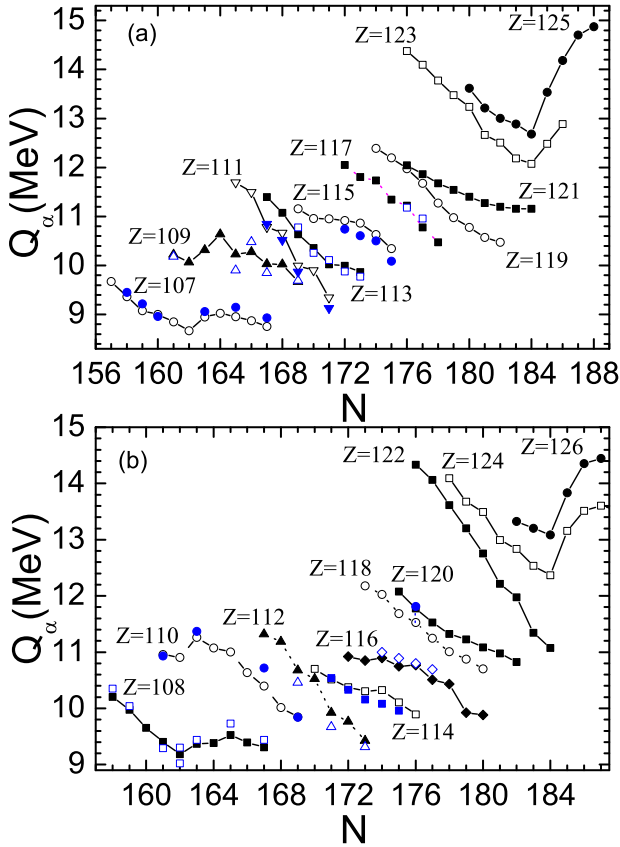


Fig. 1. (Color online) Calculated α -decay energies (symbols connected by lines) are compared with available experimental data (symbols) [1, 2, 12, 17] for even-Z (b) and odd-Z (a) nuclei with $107 \leq Z \leq 126$.

The shell corrections prevent the fission of superheavy nuclei. The height B_f of the fission barrier is mainly determined by the amplitude of the shell correction in the ground state for nuclei with $Z \geq 106$. As a result, B_f strongly depends on the neutron and proton numbers of the compound nucleus, especially, on how close they are to the magic numbers.

The results of our calculation of $B_f - B_n$ as a function of N are presented in figure 2. As it is seen, our microscopic-macroscopic approach provides the shell at $Z = 114$. However, the shell effects at $Z = 120 - 126$ are rather strong. In figure 2, the fission barrier increases when N approaches $N = 184$. Since for nuclei with $Z = 120 - 126$ the values of Q_α are minimal at $Z = 120$ (figure 2) where the fission barriers are rather high (figure 2), the nuclei with $Z = 120$ and $N = 180 - 184$ are expected to be the most stable nuclei beyond those with $Z = 114$ and $N = 176 - 178$. The shell closure at $Z = 120$ is expected in accordance with the relativistic mean-field model [18].

5 Evaporation residue cross sections

In the dinuclear system (DNS) model the dynamics of fusion is considered as a diffusion of the DNS in the mass asymmetry defined by $\eta = (A_1 - A_2)/(A_1 + A_2)$ (A_1 and A_2 are the mass numbers of the DNS nuclei) and in the internuclear distance R . The evaporation residue cross section

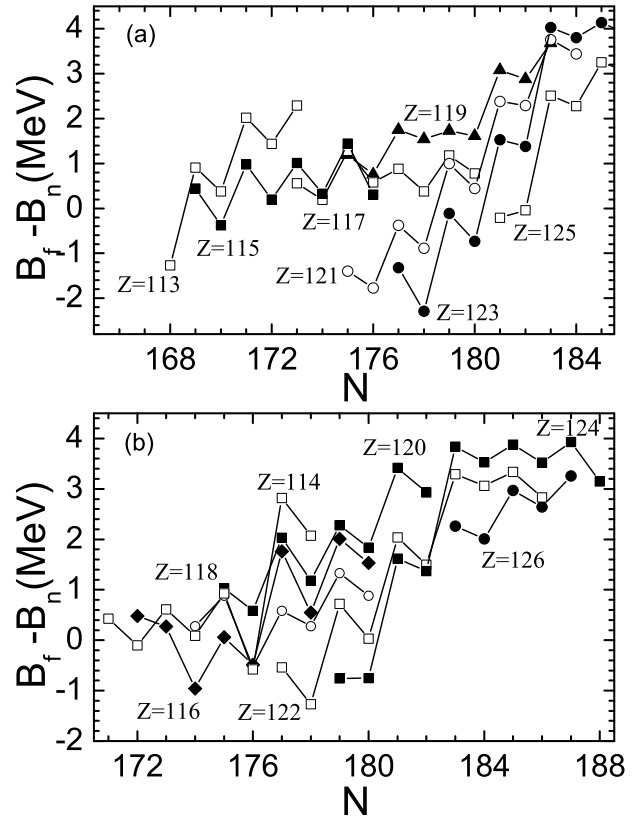


Fig. 2. The isotopic dependence of the value of $B_f - B_n$ with the data of [7]. The fission barrier B_f is assumed to be an absolute value of the shell correction in the ground state of the nucleus. The results for the isotopes related to the indicated even-Z (b) and odd-Z (a) are shown by symbols connected by lines.

in xn evaporation channel is determined as

$$\sigma_{ER}^{xn}(E_{c.m.}) = \sum_J \sigma_c(E_{c.m.}, J) P_{CN}(E_{c.m.}, J) \times W_{sur}^{xn}(E_{c.m.}, J). \quad (2)$$

The capture cross section $\sigma_c(E_{c.m.}, J)$ defines the transition of the colliding nuclei through the Coulomb barrier and the formation of the DNS when the kinetic energy above the barrier is transformed into the excitation energy of the DNS and the angular momentum J of the relative motion is redistributed in the DNS. For the reactions treated, the maximum evaporation residue cross sections are at $E_{c.m.}$ at which the collisions for all orientations of deformed nuclei become possible. Therefore, in our case there is no noticeable loss of the cross section during the capture.

Using our predictions of nuclear properties in [7], we calculated the evaporation residue cross sections in the reactions $^{48}\text{Ca}, ^{50}\text{Ti}, ^{54}\text{Cr}, ^{58}\text{Fe}, ^{64}\text{Ni} + ^{238}\text{U}, ^{244}\text{Pu}, ^{248}\text{Cm}, ^{249}\text{Cf}$ (figure 3). In comparison to our previous calculations with the mass table of Ref. [3], in figure 3 the values of σ_{ER} decrease slower with increasing Z . The stronger shell effect revealed here for nuclei with $Z > 118$ result larger survival probabilities and larger values of σ_{ER} . In the reactions $^{48}\text{Ca} + ^{238}\text{U}, ^{248}\text{Cm}, ^{249}\text{Cf}$ the experimental values of σ_{ER}^{3n} are 0.5–2.5 pb, about 1 pb, and 0.5 pb [1], respectively. Thus, the difference between the calculated and experimental σ_{ER} are within the experimental and theoretical uncertainties. A good description of existing data allows us

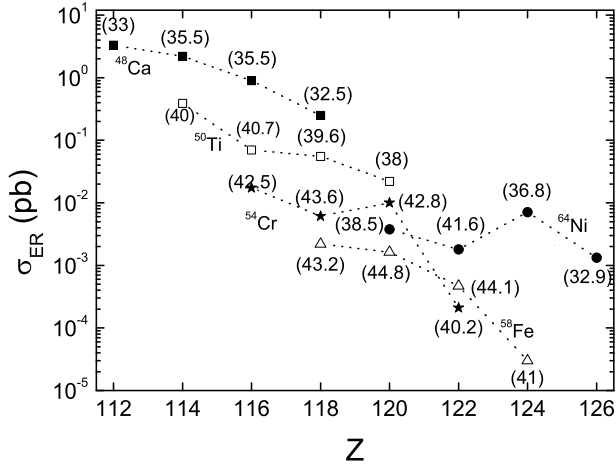


Fig. 3. The evaporation residue cross sections in the maxima of excitation functions versus charge number Z for the reactions ^{48}Ca , ^{50}Ti , ^{54}Cr , ^{58}Fe , $^{64}\text{Ni}+^{238}\text{U}$, ^{244}Pu , ^{248}Cm , ^{249}Cf . The predicted properties of superheavy nuclei from [7] are used. The excitation energies of compound nuclei are given in brackets.

to be reliable in the predictions for the reactions with projectiles heavier than ^{48}Ca .

With ^{50}Ti beam the values of σ_{ER} for the nuclei with $Z = 114 - 118$ are expected to be 5–10 times smaller than those resulted by ^{48}Ca beam. The main reason for this is the decrease of P_{CN} in Eq.(2) with mass asymmetry in the entrance channel of reaction. With ^{50}Ti the nucleus $^{295}120$ is predicted to be produced with the cross section of 23 fb. In the $^{54}\text{Cr}+^{248}\text{Cm}$ reaction the compound nucleus would have 3 neutrons more than in the $^{50}\text{Ti}+^{249}\text{Cf}$ reaction. Therefore, the decrease of P_{CN} is partly negated by the increase of W_{sur} and the nucleus $^{298}120$ can be produced with the cross section of 10 fb. For the production of nuclei with $Z = 122 - 126$, ^{64}Ni beam would lead to larger cross sections, 1–8 fb.

Using our predictions of nuclear properties, we calculated the evaporation residue cross sections of the reactions $^{50}\text{Ti}+^A\text{Cf}$ and $^{54}\text{Cr}+^A\text{Cm}$ figures 4 and 5. At zero excitation energy, the predicted values of fission barriers used in the calculations are in the energy interval 8.1–10.1 MeV. Note that for the reactions $^{48}\text{Ca}+^{238}\text{U}$, ^{244}Pu , ^{248}Cm , ^{249}Cf the calculated and experimental values of evaporation residue cross sections are quite close [19]. A good description of existing data allows us to be confident in the predictions for the reactions with heavier projectiles. In the $^{50}\text{Ti}+^{249}\text{Cf}$ ($Q=-194.75$ MeV) reaction the nucleus $^{295}120$ is predicted to be produced in a $3n$ evaporation channel with a cross section of 23 fb. In the $^{54}\text{Cr}+^{248}\text{Cm}$ ($Q=-205.59$ MeV) reaction the compound nucleus would have 3 neutrons more than in the $^{50}\text{Ti}+^{249}\text{Cf}$ reaction. Therefore, the decrease of P_{CN} is partly negated by the increase of W_{sur} , and the nucleus $^{298}120$ is predicted to be produced with a cross section of 10 fb ($4n$ evaporation channel). As in Refs. [20–22], the isotopic dependence of σ_{ER} is rather weak in the treated interval of mass numbers A . Indeed, the values of σ_{ER} are almost the same in the cases of ^{246}Cm ($Q=-208.07$ MeV) and ^{248}Cm as target. There is a certain interval of mass numbers of target nuclei where the product $P_{CN}W_{sur}$ changes only weakly [20–22].

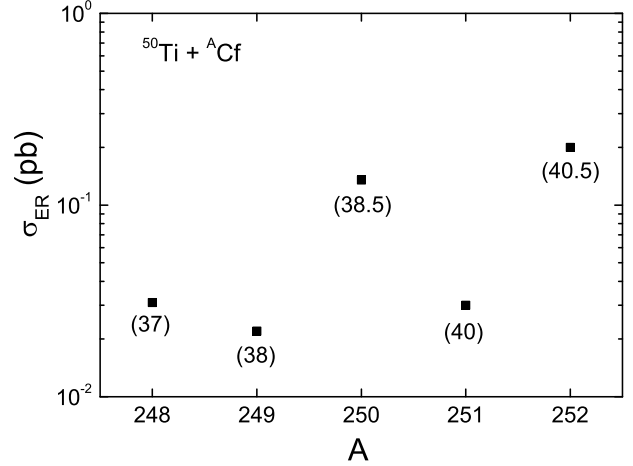


Fig. 4. Evaporation residue cross sections of the maxima of excitation functions of the reactions $^{50}\text{Ti}+^A\text{Cf}$ versus A . The excitation energies of compound nuclei are given in brackets. Ground-state mass excesses $M_{th}=211.8, 213.05, 213.76, 215.15,$ and 216.05 MeV for the nuclei $^{298}120, ^{299}120, ^{300}120, ^{301}120,$ and $^{302}120$, respectively, were used in the calculations.

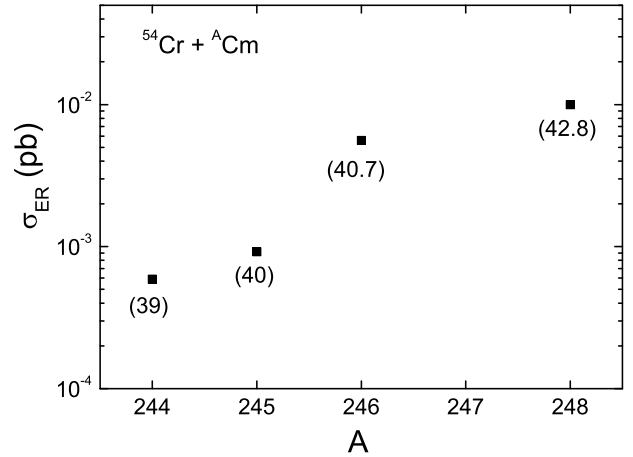


Fig. 5. The same as in figure 4, but for the reactions $^{54}\text{Cr}+^A\text{Cm}$.

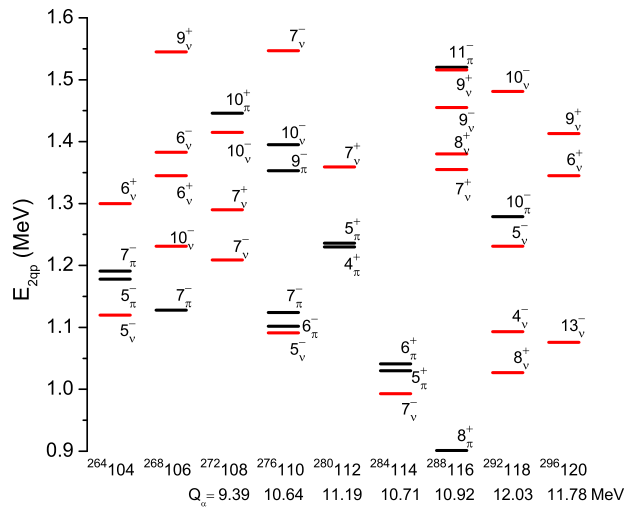


Fig. 6. Calculated energies of low-lying two-quasiproton (black signs) and two-quasineutron (red signs) states in the indicated nuclei of the α -decay chain of $^{296}120$. The resulting K values are indicated.

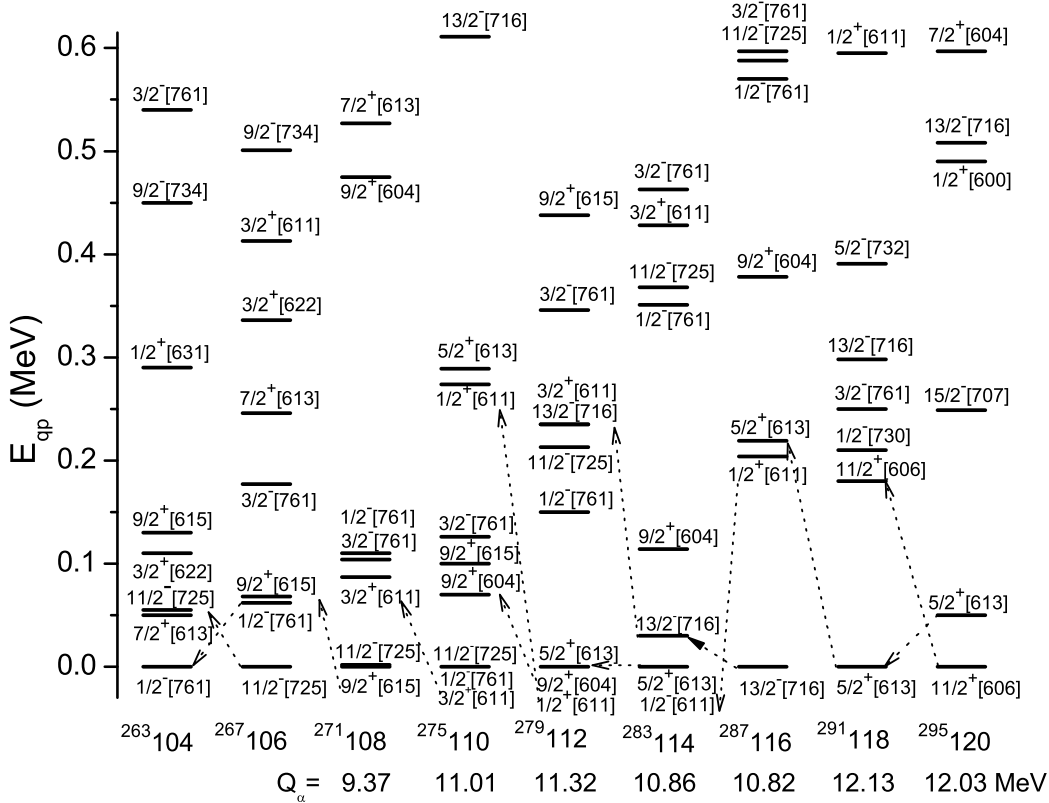


Fig. 7. Calculated energies of low-lying one-quasineutron states in the indicated nuclei of the α -decay chain of $^{295}\text{120}$. The states are marked by the Nilsson asymptotic quantum numbers. The possible α decays are shown by arrows.

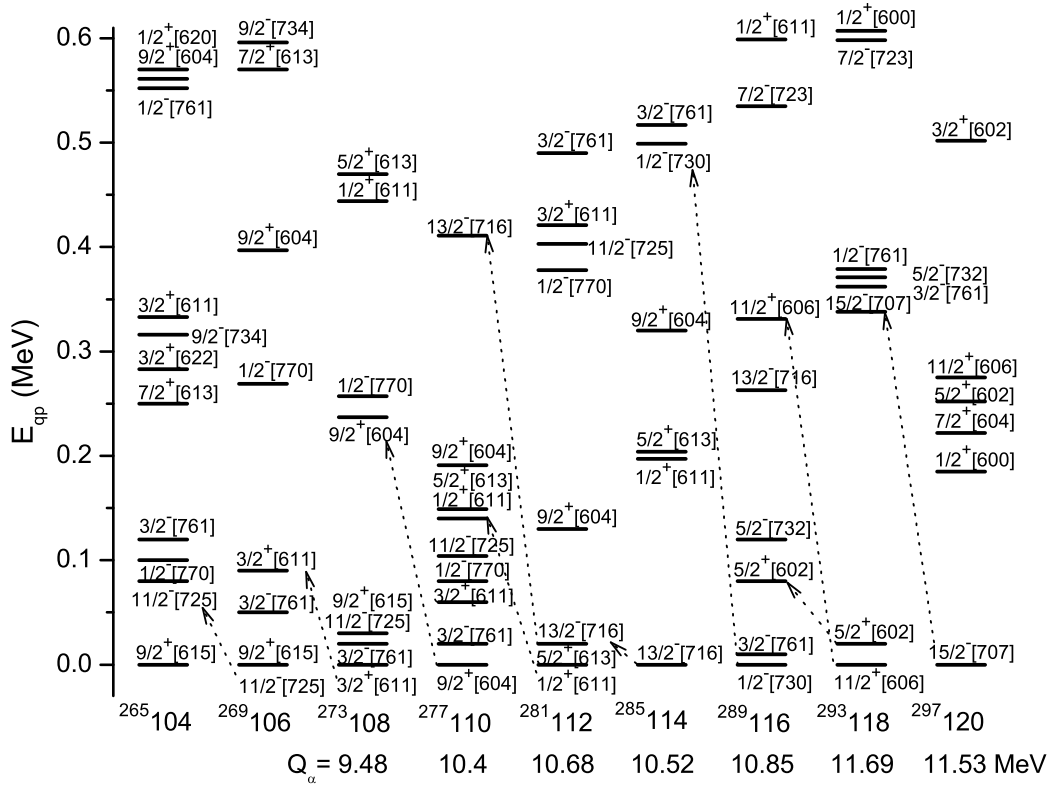


Fig. 8. The same as in figure 7, but for the nuclei of the α -decay chain of $^{297}\text{120}$.

6 One- and two-quasiparticle states

In Ref. [23] we treated the isotopes of superheavy nuclei with even Z which can be reached in complete fusion reactions with available stable projectiles and targets. The results for odd Z nuclei are given in Ref. [19].

In figure 6 the energies of two-quasiparticle states are presented for the nuclei of α -decay chain of $^{296}120$. While for nuclei with $Z \leq 118$ the first two-quasiproton states have energies smaller than 1.2 MeV, in $^{296}120$ the energies of the first two-quasiproton states are at about 1.9 MeV. This indicates a larger gap in the proton single-particle spectrum. So, the shell effects become stronger beyond $Z = 114$. The α -decay chain starting from $^{296}120$ probably terminates at $^{284}114$ by spontaneous fission. Indeed, $^{284}114$ is predicted to decay by spontaneous fission in 0.012 s [24] whereas α decay is expected to have a longer half-life of 0.045 s.

The lowest two-quasiparticle isomeric states in $^{296}120$, $^{292}118$, $^{288}116$, and $^{284}114$ are $13^-_{\nu}\{11/2^+[606] \otimes 15/2^-[707]\}$, $8^+_{\nu}\{5/2^+[602] \otimes 11/2^+[607]\}$, $8^-_{\pi}\{7/2^-[503] \otimes 9/2^-[505]\}$, and $7^-_{\nu}\{1/2^+[611] \otimes 13/2^-[716]\}$, respectively (figure 6).

The α -decay chains of $^{295,297}120$ are expected to be long, at least up to Rf, because the spontaneous fission of odd nuclei is hindered and α decays occur faster [1]. In figures 7,8 we show the calculated one-quasiparticle spectra of nuclei of α -decay chains of $^{295,297}120$. The possible α decays are marked. As seen in figure 7, the α decay of $^{291}116$ is hindered, because the corresponding levels have high energies in the daughter nucleus.

Since in figures 7,8 the nuclei with $Z > 108$ are only slightly deformed, the quasiparticle spectra are rather dense near the ground states and the appearance of isomeric states is likely. Alpha decays can occur from these isomeric states if they live longer with respect to γ decay. The α decays from the isomeric states of $^{295,297}120$ are calculated to be faster than from the ground states.

7 Summary

The calculations performed with the modified TCSM reveal quite strong shell effects at $Z = 120 - 126$. The strong shell effect is at $N = 184$. So, our macroscopic-microscopic treatment qualitatively leads to the results close to those in the mean-field treatments. The shell structure of heaviest nuclei predicted with macroscopic-microscopic model crucially depends on the parameters of single-particle potential and spin-orbit interaction. If our predictions of the structure of heaviest nuclei are correct, than one can expect the production of evaporation residues with $Z = 120$ in the reactions $^{50}\text{Ti}+^{249}\text{Cf}$ and $^{54}\text{Cr}+^{248}\text{Cm}$ with the cross sections 23 and 10 fb, respectively. The $Z = 120$ nuclei with $N = 178 - 182$ are expected to have Q_{α} about 11 MeV and life time of about 1.7 ms – 0.16 s. Note that the definition of maxima of the excitation functions provide the good test for the predictions of the models.

This work was partly supported by the DFG and RFBR.

References

1. Yu.Ts. Oganessian, J. Phys. G: Nucl. Part. Phys. **34**, R165 (2007)
2. Yu.Ts. Oganessian, *et al.*, Phys. Rev. Lett. **104**, 142502 (2010)
3. P. Möller, J.R. Nix, W.D. Myers, and W.J. Swiatecki, At. Data Nucl. Data Tables **59**, 185 (1995)
4. I. Muntian, Z. Patyk, and A. Sobiczewski, Acta. Phys. Pol. B **32**, 691 (2001); **34**, 2141 (2003); I. Muntian, S. Hofmann, Z. Patyk, and A. Sobiczewski, Acta. Phys. Pol. B **34**, 2073 (2003); Phys. At. Nucl. **66**, 1015 (2003); A. Parkhomenko, I. Muntian, Z. Patyk, and A. Sobiczewski, Acta. Phys. Pol. B **34**, 2153 (2003); A. Parkhomenko and A. Sobiczewski, Acta. Phys. Pol. B **36**, 3115 (2005)
5. G.G. Adamian, N.V. Antonenko, and W. Scheid, Phys. Rev. C **81**, 024320 (2010); Acta Phys. Pol. B **40**, 759 (2009); AIP Conf. Proc. **1165**, 136 (2009); G.G. Adamian, N.V. Antonenko, S.N. Kuklin, and W. Scheid, Phys. Rev. C **82**, 054304 (2010); G.G. Adamian, N.V. Antonenko, S.N. Kuklin, B.N. Lu, L.A. Malov, and S.G. Zhou, Phys. Rev. C **84**, 024324 (2011)
6. J. Maruhn and W. Greiner, Z. Phys. A **251**, 431 (1972)
7. A.N. Kuzmina, G.G. Adamian, N.V. Antonenko, and W. Scheid, Phys. Rev. C **85**, 014319 (2012)
8. R.-D. Herzberg and P.T. Greenlees, Prog. Part. Nucl. Phys. **61**, 674 (2008); R.-D. Herzberg and D.M. Cox, Radiochim. Acta **99**, 441 (2011)
9. F. P. Hessberger, Eur. Phys. J. D **45**, 33 (2007); F.P. Hessberger, *et al.*, Eur. Phys. J. A **41**, 145 (2009); F.P. Hessberger, *et al.*, Eur. Phys. J. A **43**, 175 (2010)
10. S. Antalic, *et al.*, Eur. Phys. J. A **43**, 35 (2010); B. Streicher, *et al.*, Eur. Phys. J. A **45**, 275 (2010); M. Venhart, *et al.*, Eur. Phys. J. A **47**, 20 (2011); S. Antalic, *et al.*, Eur. Phys. J. A **47**, 62 (2011)
11. S.K. Tandel, *et al.*, Phys. Rev. C **82**, 041301 (2010); A. Lopez-Martens *et al.*, Nucl. Phys. **A852**, 15 (2011)
12. S. Hofmann, *et al.*, Eur. Phys. J. A **32**, 251 (2007); S. Hofmann, Lec. Notes Phys. **764**, 203 (2009); Radiochim. Acta **99**, 405 (2011)
13. S. Heinz, *et al.*, J. Phys.: Conf. Ser. **282**, 012007 (2011); S. Hofmann *et al.*, Eur. Phys. J. A **48**, 62, (2012)
14. S. Hofmann and G. Münzenberg, Rev. Mod. Phys. **72**, 737 (2000)
15. S. G. Nilsson and I. Ragnarsson, *Shapes and Shells in Nuclear Structure* (Cambridge University Press, Cambridge 1995)
16. V. G. Soloviev, *Theory of Complex Nuclei* (Pergamon Press, Oxford, 1976)
17. L. Stavsetra, K.E. Gregorich, J. Dvorak, P.A. Ellison, I. Dragojević, M.A. Garcia, and H. Nitsche, Phys. Rev. Lett. **103**, 132502 (2009)
18. P.G. Reinhard, Rep. Prog. Phys. **52**, 439 (1989); P. Ring, Prog. Part. Nucl. Phys. **37**, 193 (1996); M. Bender, P.H. Heenen, and P.G. Reinhard, Rev. Mod. Phys. **75**, 121 (2003)
19. A.N. Kuzmina, G.G. Adamian, and N.V. Antonenko, Phys. Rev. C **85**, 017302 (2012)
20. G.G. Adamian, N.V. Antonenko, and W. Scheid, Phys. Rev. C **69**, 011601(R) (2004)
21. G.G. Adamian, N.V. Antonenko, and W. Scheid, Phys. Rev. C **69**, 014607 (2004)
22. G.G. Adamian, N.V. Antonenko, and W. Scheid, Phys. Rev. C **69**, 044601 (2004)

23. A.N. Kuzmina, G.G. Adamian, and N.V. Antonenko, Eur. Phys. J. A **47**, 145 (2011)
24. R. Smolańczuk, J. Skalski, and A. Sobiczewski, Phys. Rev. C **52**, 1871 (1995)